RESEARCH ARTICLE

c-Type Cytochrome Assembly Is a Key Target of Copper Toxicity within the Bacterial Periplasm

Anne Durand,[a] Asma Azzouzi,[a] Marie-Line Bourbon,[a] Anne-Soisig Steunou,[a] Sylviane Liotenberg,[a] Akinori Maeshima,[c] Chantal Astier,[a] Manuela Argentini,[b] Shingo Saito,[c] Soufian Ouchane[a]

Institute for Integrative Biology of the Cell (I2BC), CEA, CNRS UMR9198, Université Paris Sud, Gif sur Yvette 91198, France[a]; Institut de la Vision, UPMC Université Paris, UMR_S 968, Paris 75012, France[b]; Graduate School of Science and Engineering, Saitama University, Shimo-Okubo, Sakura-ku, Saitama, Japan[c]

A.D. and A.A. contributed equally to this work.

ABSTRACT **In the absence of a tight control of copper entrance into cells, bacteria have evolved different systems to control copper concentration within the cytoplasm and the periplasm. Central to these systems, the Cu^+ ATPase CopA plays a major role in copper tolerance and translocates copper from the cytoplasm to the periplasm. The fate of copper in the periplasm varies among species. Copper can be sequestered, oxidized, or released outside the cells. Here we describe the identification of CopI, a periplasmic protein present in many proteobacteria, and show its requirement for copper tolerance in *Rubrivivax gelatinosus*. The Δ*copI* mutant is more susceptible to copper than the Cu^+ ATPase *copA* mutant. CopI is induced by copper, localized in the periplasm and could bind copper. Interestingly, copper affects cytochrome *c* membrane complexes (*cbb*$_3$ oxidase and photosystem) in both Δ*copI* and *copA*-null mutants, but the causes are different. In the *copA* mutant, heme and chlorophyll synthesis are affected, whereas in Δ*copI* mutant, the decrease is a consequence of impaired cytochrome *c* assembly. This impact on *c*-type cytochromes would contribute also to the copper toxicity in the periplasm of the wild-type cells when they are exposed to high copper concentrations.**

IMPORTANCE **Copper is an essential cation required as a cofactor in enzymes involved in vital processes such as respiration, photosynthesis, free radical scavenging, and pathogenesis. However, copper is highly toxic and has been implicated in disorders in all organisms, including humans, because it can catalyze the production of toxic reactive oxygen species and targets various biosynthesis pathways. Identifying copper targets, provides insights into copper toxicity and homeostatic mechanisms for copper tolerance. In this work, we describe for the first time a direct effect of excess copper on cytochrome *c* assembly. We show that excess copper specifically affects periplasmic and membrane cytochromes *c*, thus suggesting that the copper toxicity targets *c*-type cytochrome biogenesis.**

Received 19 June 2015 **Accepted** 4 August 2015 **Published** 22 September 2015

Citation Durand A, Azzouzi A, Bourbon ML, Steunou AS, Liotenberg S, Maeshima A, Astier C, Argentini M, Saito S, Ouchane S. 2015. *c*-type cytochrome assembly is a key target of copper toxicity within the bacterial periplasm. mBio 6(5):e01007-15. doi:10.1128/mBio.01007-15.

Editor Howard A. Shuman, University of Chicago

Address correspondence to Soufian Ouchane, soufian.ouchane@i2bc.paris-saclay.fr.

Copper is required as a redox cofactor in many enzymes involved in vital metabolisms. Only traces of copper are needed to fulfill its role. Copper is highly toxic even at low concentrations and promotes oxidative damage or degradation of solvent-exposed 4Fe-4S centers (1), leading to impaired cell functioning and cell death. Accumulation of copper in the cytoplasm may also interfere with the formation of iron-sulfur clusters, as suggested in reference 2. In Gram-negative bacteria, all cuproenzymes are located within the inner membrane and the periplasm, which implies transport of copper from the medium or from the cytoplasm to these cell compartments. Copper diffuses through nonspecific outer membrane porins into the periplasm and transits to the cytoplasm (3). Copper can also be supplied from the cytoplasm to the periplasmic and inner membrane proteins through specific copper ATPases (4–6). In all subcellular compartments, copper presents a threat to the cell integrity; therefore, it has to be handled by specific copper homeostasis systems to avoid its toxicity. For that purpose, bacteria have acquired different systems to tightly control the copper concentration. Among these systems, a well-studied copper induced efflux system was described in *Escherichia coli*. The system includes the transcriptional regulator CueR, which senses Cu ions in the cytoplasm and triggers the response by inducing the expression of *copA* and *cueO* genes, coding for the P_{1B}-1-type ATPase (CopA) and the periplasmic multicopper oxidase (CueO), respectively (7, 8). CopA is required for removing excess Cu from the cytoplasm to the periplasm (9), where CueO oxidizes Cu(I) under aerobic conditions to less toxic Cu(II) (10). Excess copper can also be removed from the periplasm and released outside the cell by the CusF/CusCBA system, which has been identified in only few species and studied solely in *E. coli* (11, 12). In contrast, the P_{1B}-1-type ATPase CopA is found in almost all proteobacteria, and *copA* mutations result in increased sensitivity to copper (13).

In addition to these systems, other periplasmic proteins that

are or may be involved in copper handling were found in many bacteria, such as PcoC and PcoE in *E. coli* (14), CopG, CopK, and CzcE in *Cupriavidus metallidurans* (15, 16), CueP in *Salmonella enterica* serovar Typhimurium (17, 18), CucA and CinA in *Pseudomonas putida* (19), and CopM in *Synechocystis* strain PCC 6803 (20, 21). This variety and multiplicity of proteins highlight their essential role to protect cells from the periplasmic highly toxic reduced Cu(I). To avoid the toxic effect of copper ions in the periplasm, some of these proteins can either (i) oxidize copper (CueO and CuiD in *S.* Typhimurium or CutO in *Rhodobacter capsulatus*) (10, 22, 23), (ii) sequester copper ions (PcoC and CopC in *E. coli* and CueP in *S.* Typhimurium) (14, 18), or (iii) deliver copper ions to outer membrane exporter to remove the metal outside the cell (CusF in *E. coli*) (7, 12).

In the purple photosynthetic bacteria *R. capsulatus* and *Rhodobacter sphaeroides*, the mechanisms and the whole copper efflux system are not yet characterized in detail (23, 24). In *Rubrivivax gelatinosus*, the roles of the P_{1B} ATPases CtpA and CopA as a copper delivery protein to membrane cuproproteins and as a copper efflux pump required for copper tolerance, respectively, were reported (5, 25). In the *copA*-null mutant, excess copper affects the cytoplasmic pathway of heme and chlorophyll biosynthesis, by decreasing heme- and/or chlorophyll-containing complexes within the membrane (25, 26). It was reported that in *R. gelatinosus* (25) and in the human pathogen *Neisseria gonorrhoeae* (27), copper seems to poison HemN, likely by degradation of its exposed 4Fe-4S cluster.

To further characterize the copper tolerance system in *R. gelatinosus*, we performed protein profile analyses and identified the copper-induced periplasmic protein CopI. Genetic and physiological analyses of the Δ*copI* mutant showed that CopI plays a major role in copper tolerance. Over a span of decades, intensive research provided evidence supporting excess-Cu-induced disorders in all organisms (28). DNA damage and reactive oxygen species generation are among the mechanisms by which copper inhibits or kills overloaded cells (28). Our findings pinpoint cytochrome *c* assembly as a new target of copper that could contribute to its toxicity and demonstrate the crucial role of copper detoxification within the periplasm.

RESULTS

CopI is a copper-induced putative periplasmic protein. To identify new copper-handling proteins involved in copper homeostasis in *R. gelatinosus*, the wild-type (WT) strain was subjected to copper stress (1.2 mM $CuSO_4$) under anaerobic photosynthetic (PS) conditions. Copper-dependent induction of soluble proteins was assessed after Coomassie blue-stained SDS-PAGE. While exposure to copper stress did not affect cell viability, it significantly changed the protein expression profile compared to control conditions (Fig. 1A). Two major intense bands (17 and 14 kDa) were differentially detected in the soluble fraction of copper-stressed bacteria (Fig. 1A). Protein identification of these bands was performed by nano-liquid chromatography tandem mass spectrometry (nano-LC-MS/MS) after in-gel trypsin digestion of excised bands. To assess the specificity of copper-induced protein expression, gel slices of identical sizes were also excised from the soluble protein fraction of unstressed bacteria. Comparative analyses of Mascot search results showed that CopI (17 kDa) and CopJ (14 kDa) were specifically identified under copper stress conditions. While the number of identified peptides (CopI, 5; CopJ, 7) and protein coverage (CopI, 44%; CopJ, 69%) were acceptable, N-terminal characterization was rather poor. Since predicted signal peptides (SignalIP and SMART) for periplasm localization are present in sequences of both proteins, we reviewed the LC-MS/MS datasets using the Mascot Error Tolerant Search software to identify nontryptic peptides. N-terminally processed CopJ peptides could not be found, whereas the CopI peptide $_{23}$DAGHDHGSAH AGAHAHDADTPYGRPGDAAK$_{52}$ was unambiguously identified (Fig. 1B), thus confirming that CopI was N-terminal processed and that the protein is most probably localized in the periplasm.

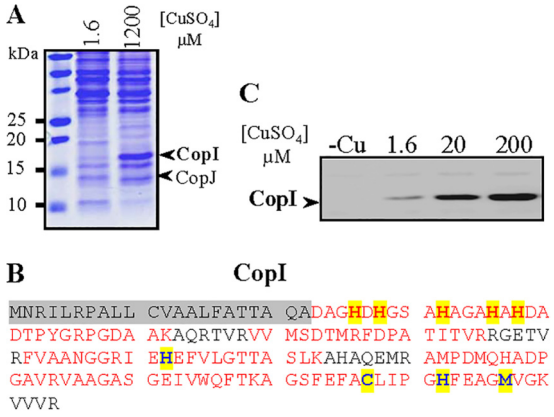

FIG 1 (A) Copper-dependent induction of soluble proteins in the WT strain grown under PS conditions in malate containing 1.6 μM CuSO4 or in malate supplemented with 1.2 mM CuSO4. (B) CopI sequence. The CopI peptides identified by MS are in red. The signal peptide and the His-rich sequence are highlighted in grey and in yellow, respectively. Residues of the CopI putative copper binding motif (H70C125H130M135) are blue and highlighted in yellow. (C) Expression of CopI in the WT soluble fraction. Cells were grown under PS conditions in the absence of copper (−Cu) and in the presence of increasing CuSO4 concentrations. Equal amounts of soluble protein were loaded on SDS-PAGE gels and then transferred for CopI detection using the HRP-HisProbe.

Protein sequence analyses revealed a plastocyanin-like fold with a conserved copper binding motif ($H_{70}C_{125}H_{130}M_{135}$) within CopI and a $C_{18}XXC_{21}$ sequence within CopJ, a motif potentially involved in copper binding. CopI and CopJ are encoded by *copI* and *copJ*, located immediately downstream of the *copAR* locus, which is involved in copper tolerance in *R. gelatinosus*, suggesting that these proteins may be required for copper tolerance.

Because of the presence of five histidines within the mature CopI sequence (Fig. 1B), CopI expression could be detected specifically on Western blots using the horseradish peroxidase (HRP)-conjugated HisProbe. Thus, Western blotting of soluble fractions of WT strain grown anaerobically by photosynthesis under different copper concentrations was performed. CopI was not detected in the control (copper-depleted medium) or in the *copI* deletion strain (see below for descriptions of mutants); however, when the copper concentration was increased from 1.6 to 200 μM, CopI amount increased concomitantly (Fig. 1C) in agreement with the RT-PCR data (see Fig. S1 in the supplemental material). These data confirm that CopI is induced by excess copper. In addition, as for CopA expression (25), we showed that full induction of CopI requires the presence of the copper regulator CopR (see Fig. S1).

CopI is located in the periplasm. Since mass spectrometry analysis showed that CopI protein is N-terminally processed and

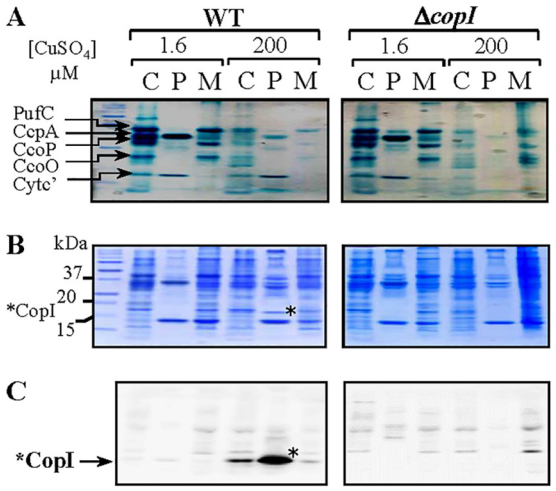

FIG 2 Cellular localization of CopI. WT and Δ*copI* cells were grown under microaerobic conditions in the presence of 1.6 and 200 μM $CuSO_4$. (A) Cellular fractions (C, total fraction; P, periplasm; M, membranes) were separated on 12% SDS–PAGE, and the *c*-type cytochromes were revealed by TMBZ staining. (B) These gels were subsequently stained with Coomassie blue to detect CopI (*) in the periplasmic fraction of WT strain exposed to $CuSO_4$. (C) CopI was revealed specifically on Western blots using the HRP-HisProbe.

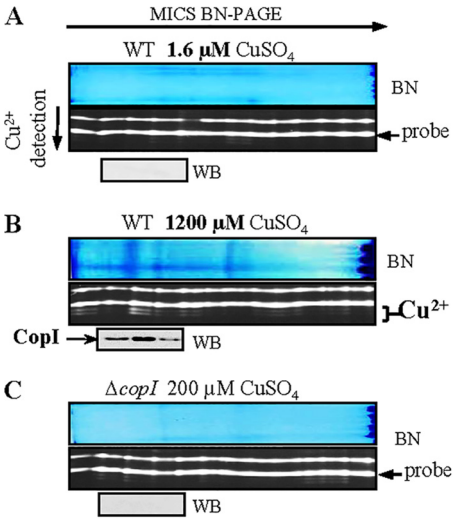

FIG 3 Detection of copper-binding proteins by MICS-BN-PAGE followed by copper ion detection PAGE. Each panel is divided into three parts. The top shows MICS-BN-PAGE (BN). The middle shows copper detection by PAGE for the whole BN lane; the probe complexed to copper is indicated (Cu^{2+}), while the two upper signals correspond to Ca probe and free probe (probe). At the bottom is the Western blot (WB) of electroeluted protein from the MICS-BN-PAGE for CopI detection. (A) WT grown in 1.6 μM $CuSO_4$; (B) WT in medium supplemented with 1.2 mM $CuSO_4$; (C) the Δ*copI* strain grown in 200 μM $CuSO_4$. In panels A and C, no Cu^{2+}-probe complex or CopI could be detected, while in panel B, in which CopI is induced, CopI and the Cu^{2+}-probe complex are detected and colocalize in the same fractions.

is likely a periplasmic protein, we isolated an enriched periplasmic fraction from intact WT *R. gelatinosus* and Δ*copI* mutant (see below) cells grown under 1.6 μM or 200 μM $CuSO_4$ stress to localize CopI. As a control for the isolation procedure (see Materials and Methods), we analyzed membrane and soluble periplasmic *c* type cytochromes in each isolated fraction by specific 3,3′,5,5′-tetramethylbenzidine (TMBZ) staining. In the periplasmic fractions of WT and the Δ*copI* strain grown in the presence of 1.6 μM $CuSO_4$, two major cytochromes *c* corresponding to the soluble periplasmic *c* type cytochromes *c*′ and the cytochrome *c* peroxidase CcpA were detected (Fig. 2A), whereas the membrane *c* cytochromes (CcoP, CcoO, and PufC) were present mainly in the membrane fraction. The two soluble cytochromes *c* were strongly reduced in cells grown in the presence of 200 μM $CuSO_4$. Interestingly, Coomassie blue staining revealed the presence of a 17-kDa protein band only in the periplasmic fractions of WT cells challenged with excess copper (Fig. 2B). The presence of CopI in this later fraction was unambiguously confirmed by Western blotting (Fig. 2C), and a smaller amount of CopI was detected in the total fraction.

CopI protein could bind copper. Since CopI harbors a plastocyanin-like fold with a conserved copper binding motif and a cluster of 5 scattered histidines susceptible to bind transition metals like copper, we used the method of metal ion contaminant sweeping-blue native polyacrylamide gel electrophoresis (MICS-BN-PAGE) and a fluorescent probe (29) to map copper binding proteins in soluble fractions from WT cells grown microaerobically with 1.6 or 1,200 μM $CuSO_4$ compared with Δ*copI* mutant cells grown with 200 μM $CuSO_4$. While no band was observed in the first BN-PAGE dimension for WT and Δ*copI* samples incubated, respectively, with 1.6 and 200 μM $CuSO_4$ (Fig. 3A and C), distinct protein bands were observed in the WT cells grown with 1,200 μM $CuSO_4$ (Fig. 3B). Subsequently, the copper content in each cut band was measured after acid extraction and addition of a fluorescence probe (FTC-ABDOTA); the resulting metal-probe complex was separated by PAGE (29). A strong copper signal was observed only in extracts of WT cells grown with 1,200 μM $CuSO_4$ (Fig. 3B). The percentage of copper in the selected cut band relative to total copper concentration in the entire lane of the gel was calculated as 76% ± 19% ($n = 6$). No copper ions were detected in the gel fractions corresponding to the same positions for Δ*copI* and WT samples incubated with 200 and 1.6 μM $CuSO_4$, respectively. This strongly implies that the isolated protein at this position formed stable (inert) complexes with copper ions. To determine whether CopI was thus present in these bands, the proteins were electroeluted from the MICS-BN-PAGE and subjected to Western blotting for CopI detection. CopI was detected only in the gel fractions where a high concentration of copper was detected, i.e., in WT cells grown with 1,200 μM $CuSO_4$ (Fig. 3). Accordingly, these data strongly suggest that CopI strongly binds copper in the periplasm.

CopI is required for copper resistance under both aerobic and anaerobic conditions. A *copI* deletion strain was constructed to analyze the role of CopI in copper homeostasis. The copper sensitivity of the Δ*copI* strain was investigated by growing the strain with increasing $CuSO_4$ concentrations in comparison with the WT and the *copA* mutant. First, on solidified medium, growth of both Δ*copI* and *copA* strains was affected at 120 μM and inhibited beyond 300 μM $CuSO_4$ with aerobic respiration, unlike the WT (Fig. 4A). Under anaerobic PS conditions, the growth of the Δ*copI* mutant was inhibited at 80 μM $CuSO_4$, whereas growth of the *copA* mutant was unaffected by this $CuSO_4$ concentration (Fig. 4A). Second, growth inhibition by $CuSO_4$ of these strains was performed in liquid medium in the presence of increasing copper concentrations under both respiration and anaerobic PS conditions (Fig. 4B). Under both conditions, growth of Δ*copI* and *copA*

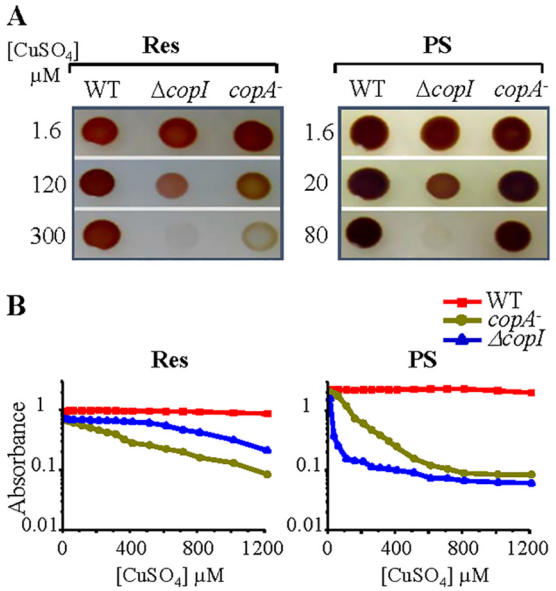

FIG 4 Growth phenotype and cell viability of the WT, Δ*copI* mutant, and *copA* mutant grown with increasing copper concentrations. (A) Cells were grown in the dark with aerobic respiration (Res) (1.6 to 300 μM $CuSO_4$) or anaerobically by PS (1.6 to 80 μM $CuSO_4$) on plates for 48 h at 28°C prior to photography. (B) Copper tolerance was assayed for the WT, *copA*, and Δ*copI* strains. Cells (initial optical density at 680 nm [OD_{680}], 0.02) were grown in liquid by Res or by PS in the presence of different $CuSO_4$ concentrations, and absorbance at 680 nm was measured after 24 h.

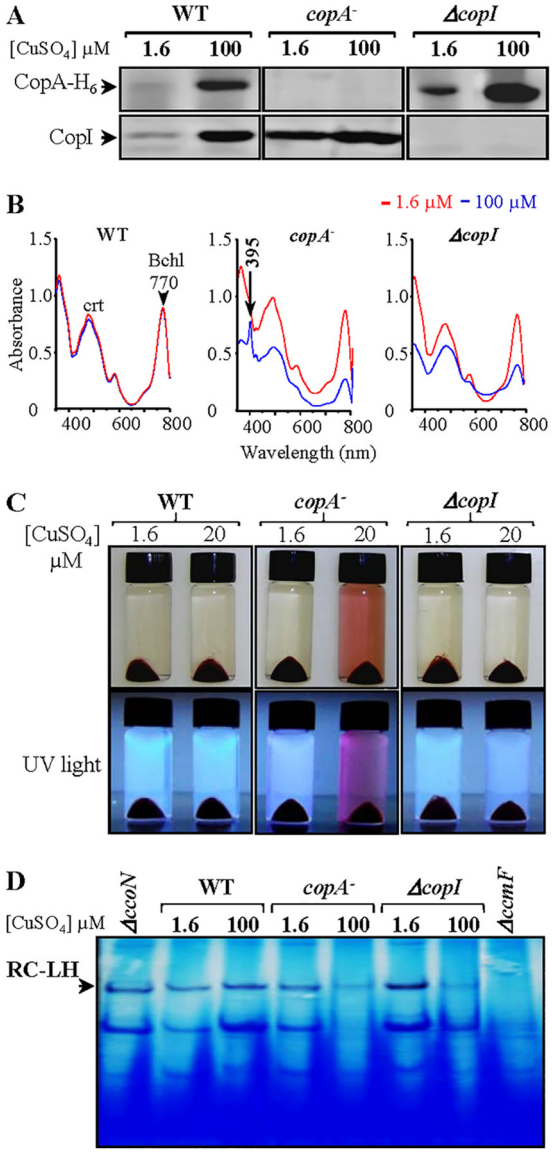

FIG 5 (A) Expression level of CopA and CopI in different genetic backgrounds. Equal amounts of proteins from WT $CopAH_6$, Δ*copI* $CopAH_6$, and *copA* mutants were analyzed by Western blotting using the HRP-HisProbe. (B) Absorption spectra of total pigment extracts from WT, Δ*copI*, and *copA* cells grown in malate or with 100 μM $CuSO_4$. Pigments were extracted from the same amount of cells (1 OD_{680} unit). (C) Copper-dependent release of coproporphyrin III in the culture medium of grown cells. Phenotype of the Δ*copI* mutant in comparison with the WT and the *copA* mutant grown in liquid malate or malate supplemented with 20 μM $CuSO_4$. Cultures were centrifuged to reveal the presence of the UV-fluorescent pigment identified previously as coproporphyrin III (25) only in the spent medium of the *copA* mutant grown in the presence of 20 μM $CuSO_4$. (D) Comparison of the amount of photosystem (RC-LH) in the solubilized membrane fractions of the WT, Δ*copI*, and *copA* strains. Equal amounts of DDM-solubilized membranes were separated on 3-to-12% gradient BN-PAGE.

mutants was reduced when they were exposed to $CuSO_4$, while the WT strain was unaffected (Fig. 4B). Under aerobic respiration (Res) conditions, the *copI* mutant was less affected than the *copA* mutant, in contrast with the solid agar plate data. This may be due to the difference in oxygen tension between plates and shaken liquid cultures. Under PS anaerobic conditions, the Δ*copI* mutant was extremely sensitive to copper, as its growth was inhibited at 50 μM $CuSO_4$, similar to the data obtained on solid agar plates. Growth of the *copA* strain was also reduced, as observed under aerobic conditions. Finally, WT copper tolerance could be restored in the Δ*copI* mutant by an ectopic copy of *copI*, showing that the phenotype was not due to polar effects of the cassette insertion on the downstream *copJ* gene (see Fig. S2 in the supplemental material). These data demonstrate that CopI is required for copper resistance under both aerobic and anaerobic conditions and that the Δ*copI* strain is more sensitive to copper than the *copA* strain under anaerobic conditions. Moreover, disc diffusion assay results confirmed that the Δ*copI* strain is extremely susceptible to copper under anaerobic photosynthesis conditions relative to the *copA* mutant (see Fig. S2). Altogether, the results showed that CopI is critical when oxygen tension drops.

Expression of CopI does not require the expression of the efflux pump CopA. The increased sensitivity to copper of the Δ*copI* mutant originates from the deletion of *copI*. However, this phenotype could also indirectly result from impaired expression or a complete lack of expression of the copper efflux pump ATPase CopA. To rule out this hypothesis, the *copI* gene was also deleted in a WT strain harboring the His-tagged *copA* construct on the chromosome to monitor the expression of CopA in the absence of CopI.

The expression of $CopA\text{-}H_6$ and CopI was monitored in WT and Δ*copI* strains containing the $CopA\text{-}H_6$ construct and the *copA* strains grown microaerobically in malate medium (1.6 μM) or in 100 μM $CuSO_4$-supplemented medium. CopI and $CopA\text{-}H_6$ were not detected in the fractions from the respective mutants (Fig. 5A). $CopA\text{-}H_6$ was present in the membranes of the Δ*copI* mutant under both experimental conditions, and the amount of

CopA-H_6 was even higher in the Δ*copI* mutant than in the WT (CopA-H_6) control strain. This indicates that the observed phenotype in the Δ*copI* mutant was not related to a decrease in the expression of CopA. The increase of CopA protein within Δ*copI* mutant membranes may be due to a loss of copper control within the periplasm, resulting in an overloading of the cytoplasm with copper, which in turn induces the expression of the efflux pump CopA. Expression of CopI in the absence of the ATPase CopA was also checked in the *copA* strain. The results showed a constitutive expression of CopI in the *copA* mutant, while in the WT (CopA-H_6), CopI expression was induced by copper. Because in the *copA* strain, copper accumulates within the cytoplasm, the copper sensor CopR induces CopI expression (see Fig. S1 in the supplemental material).

To demonstrate that the expression of CopI in *copA* mutant and of CopA in the Δ*copI* mutant contributes to copper tolerance, a *copA* Δ*copI* double mutant was generated, and copper resistance was assayed on agar plates in comparison with that of the *copA* and Δ*copI* single mutants. Unlike the single mutants, the double mutant could not grow beyond 120 μM $CuSO_4$ under aerobic conditions and 20 μM $CuSO_4$ during anaerobic photosynthesis (see Fig. S3 in the supplemental material). The double mutant is extremely copper sensitive, indicating that the proteins expressed in the single mutants contribute individually to copper tolerance.

Mutations in *copI* and *copA* affect the photosystem and the cytochrome *c* oxidase *cbb*$_3$, but through different mechanisms. In two recent reports, we showed that excess copper affects the tetrapyrrole biosynthesis pathway in *copA* mutant and thereby affects the assembly of heme- and chlorophyll membrane-containing complexes, such as the *cbb*$_3$ cytochrome *c* oxidase and the photosystem (25, 26). We therefore questioned whether deletion of *copI* can give rise to the same phenotype. First, we visually compared the photosynthetic pigment content of the cells grown under microaerobic conditions with two copper concentrations. In contrast to the WT and *copA* strains, the Δ*copI* culture exhibited different pigmentation at 100 μM $CuSO_4$ (data not shown). Then, the pigment content of each culture was analyzed by UV-visible (UV-Vis) absorption. In the Δ*copI* and *copA* cells, the bacteriochlorophyll (peak at 770 nm) and carotenoid (430 to 520 nm) contents were reduced when copper concentration was increased, in sharp contrast with the WT, where the photopigments were not affected (Fig. 5B). Interestingly, in Δ*copI* cells and medium, no trace of coproporphyrinogen III (peak at 395 nm) was observed, in sharp contrast with *copA* cells (Fig. 5B and C), as previously reported by Azzouzi et al. (25). A decrease in the amount of the photosystem (RC-LH [reaction centre-light harvesting]) was also observed on BN-PAGE for both Δ*copI* and *copA* strains grown in the presence of excess copper (Fig. 5D).

As for photosynthesis, excess copper results in slower microaerobic growth in the Δ*copI* strain (data not shown). Since the *cbb*$_3$ oxidase is required for microaerobic respiration (30), we questioned whether the cytochrome *c cbb*$_3$ oxidase is affected when copper handling in the periplasm is deregulated in the Δ*copI* mutant. Comparable DAB (3,3′-diaminobenzidine)-positive bands on BN-PAGE corresponding to the *cbb*$_3$ oxidase activity were observed in the WT native membranes regardless of the copper concentration (Fig. 6A). In contrast, in the *copA* and Δ*copI* membranes, the amount of active *cbb*$_3$ was decreased when copper concentration increased to 100 μM. Concomitantly with the decrease in the oxidase activity, the catalytic CcoN and the two cytochrome *c*-type CcoO and CcoP subunits of *cbb*$_3$ oxidase were decreased, as shown on Western blots (Fig. 6B). Interestingly, solely in the membranes of the *copA* strain, additional bands corresponding to the proteolysis of CcoP (lower band) and CcoO (upper bands) were observed.

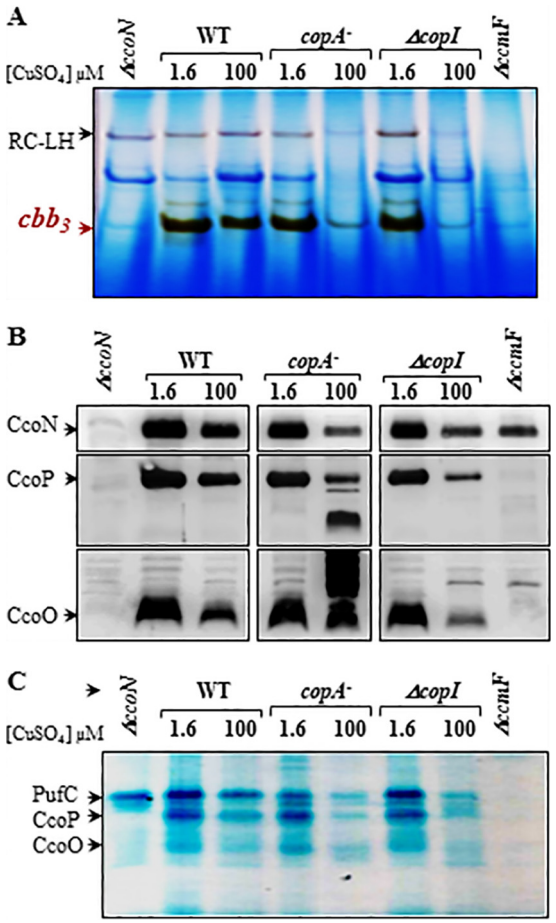

FIG 6 (A) *cbb*$_3$ oxidase in-gel activity assay on BN-PAGE gradient. DAB staining was used to detect the *cbb*$_3$ oxidase activity. (B) Detection of *cbb*$_3$ subunits by Western blotting. The *cbb*$_3$ CcoN, CcoO, and CcoP subunits were revealed in these membranes using specific antibodies raised against these subunits. (C) Detection of *c*-type cytochromes. The *c*-type cytochromes were revealed in the presence of TMBZ. For both panels B And C, equal amounts of membrane proteins from the WT and mutants were separated on 12% SDS–PAGE.

These data demonstrate that as for the *copA* strain, excess copper also affects the amount of the *cbb*$_3$ cytochrome *c* oxidase within the membranes in the Δ*copI* strain.

The photosystem and *cbb*$_3$ oxidase decrease accounts for the slower PS and microaerobic growth of both mutants and could be explained by the effect of copper on cytoplasmic porphyrin synthesis in *copA* but not in the Δ*copI* mutant. We suggest that in the Δ*copI* strain, copper is removed from the cytoplasm by the efflux pump CopA, thus protecting the cytoplasmic steps of the tetrapyrrole biosynthesis pathway from toxic excess copper, and that copper may affect yet-unknown periplasmic processes.

Excess copper in the Δ*copI* strain affects cytochrome *c* membrane complexes. We also analyzed the presence of *c*-type cytochromes by TMBZ staining in membrane fractions. A significant

decrease of all membrane *c*-type cytochromes, including the tetraheme cytochrome *c* (PufC) subunit of the reaction center (RC) and the two cytochrome *c* subunits (CcoO and CcoP) of cbb_3, was observed for both Δ*copI* and *copA* strains grown in the presence of excess copper (Fig. 6C). As expected, no *c*-type cytochrome could be detected in membranes of the Δ*ccmF* strain affected in the cytochrome *c* biogenesis pathway, and only a slight effect was observed for the WT. We had also observed a decrease in periplasmic *c*-type cytochromes (Fig. 2A). These data suggest that excess copper affects both periplasmic and membrane *c*-type cytochromes in these mutants. Nevertheless, in the *copA* strain, copper accumulates within the cytoplasm, and the decrease of *c*-type cytochromes results from a decrease of heme synthesis; consequently, both heme *b*- and *c*-containing complexes should be affected. In contrast, in the Δ*copI* strain, copper should accumulate within the periplasm and may affect only *c*-type cytochrome assembly because covalent binding of heme *b* to the apocytochromes takes place within the periplasm (31). To test this assumption, we subsequently analyzed the effect of excess copper on the activity of succinate dehydrogenase (Fig. 7A), a heme *b* membrane complex devoid of *c*-type cytochromes. Interestingly, in contrast to cbb_3 oxidase activity, the activity of this complex was not detectably diminished in the Δ*copI* strain in the presence of excess copper, strongly suggesting that only heme *c*-type complex assembly is adversely affected by excess copper in this strain. The specificity of this signal was proved by loss of signal after addition of malonate (an inhibitor of succinate dehydrogenase) (data not shown). It is of note that in the *copA* mutant, the activity of succinate dehydrogenase was not affected, although the complex contains 4Fe-4S centers. These centers are protected from copper because they are occluded by polypeptides in the complex and thus are not exposed.

Therefore, these in-gel activities and the absence of heme intermediate accumulation in the Δ*copI* strain strongly suggest that in the Δ*copI* mutant, the heme *b* biosynthesis pathway is unaffected, in sharp contrast with the *copA* mutant.

To further confirm these data, we performed redox spectral analyses (reduced minus oxidized spectra) to assess the cytochrome *c* (peak at 552 nm) and *b* (peak at 560 nm) ratios present in these membranes (Fig. 7B). Comparable spectra were recorded for the WT, *copA*, and Δ*copI* membranes from cells grown in 1.6 μM $CuSO_4$. Addition of 100 μM $CuSO_4$ resulted in a slight decrease of heme *c* and *b* in the WT. This decrease was more pronounced in the *copA* membranes, yet both heme *c* and *b* are present in these membranes, as judged by the 552- and 560-nm peaks. Interestingly, in the Δ*copI* membranes, a significant decrease of the 552-nm peak was observed, demonstrating an overall decrease of *c*-type cytochromes within the Δ*copI* cells. As controls, *c*- and *b*-type cytochromes were also monitored in membranes isolated from Δ*ccmF* and Δ*ccoN* strains, affected, respectively, in the cytochrome *c* biogenesis pathway and the cbb_3 catalytic subunit CcoN.

c-type cytochrome assembly is a primary target of copper toxicity within the periplasm. When low excess copper (100 μM) is present in the medium, the Δ*copI* strain produces less *c*-type cytochromes. Because very high copper concentrations (1 to 2 mM) slow growth and also are toxic for the WT strain with no accumulation of heme intermediates, we assumed that high copper concentrations may also affect *c*-type cytochrome assembly in the WT background. To provide evidence, we monitored cytochrome *c* and *b* ratios present in total extract of WT cells exposed to increasing concentrations of $CuSO_4$ (1.6 to 1,500 μM) in comparison with Δ*copI* and *copA* mutants (Fig. 7C and 8). The data clearly show a shift in the spectra, with cytochrome *c* present at low copper concentrations, while at high copper concentrations, the 552-nm peak decreased and the main peak detected corresponds to that of heme *b* (560 nm), indicating a gradual decline in the amount of *c*-type cytochromes in the WT membranes when cells are exposed to a high copper concentration. In the Δ*copI* extracts, the effect of excess copper on cytochrome *c* content was observed early at a low $CuSO_4$ concentration (25 μM), and the effect was more drastic when cells were challenged with higher copper concentrations (Fig. 8). For the *copA* mutant, cells were challenged with increasing nonlethal concentrations up to 250 μM. As expected, the spectra show a decrease of both cytochrome *c* and *b* contents (Fig. 8), and the main peak detected corresponds to that of cytochrome *c*.

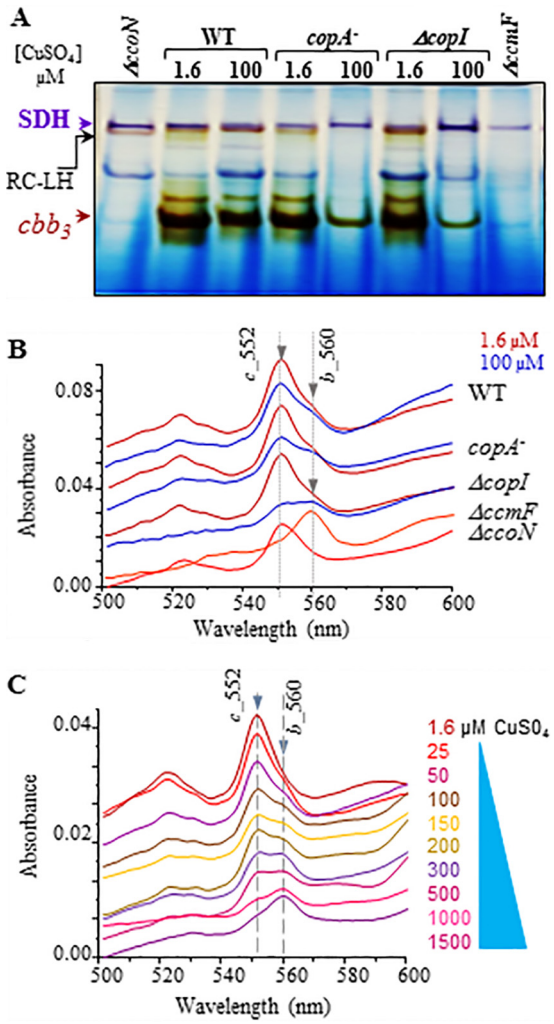

FIG 7 (A) Succinate dehydrogenase (SDH) in-gel activity assay. The membranes on BN-PAGE assayed for cbb_3 oxidase (Fig. 6A) were subsequently assayed for SDH activity. (B) Difference (reduced minus oxidized) spectra of WT, Δ*copI*, and *copA* membranes from cells grown in 1.6 μM (red) or 100 μM (blue) $CuSO_4$. Δ*ccoN* and Δ*ccmF* strains were grown only in 1.6 μM $CuSO_4$. (C) Difference spectra of total fractions from WT grown in the presence of increasing copper concentrations.

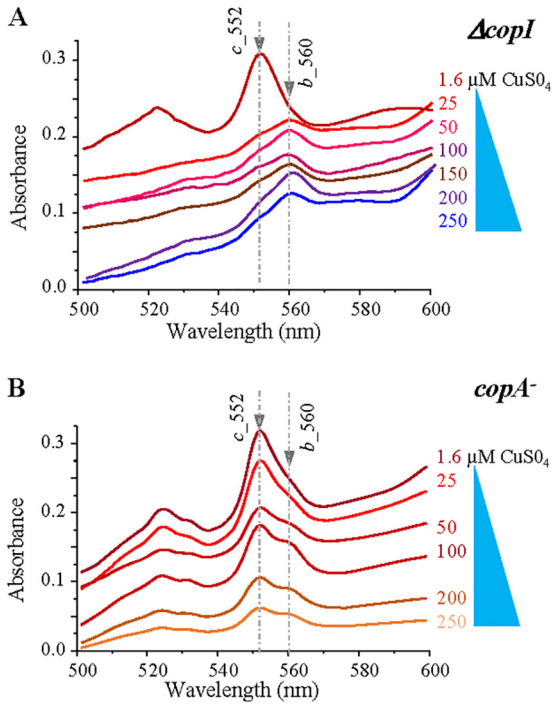

FIG 8 Difference in total *b*- and *c*-type cytochrome content between Δ*copI* and *copA* mutants. Difference (reduced minus oxidized) spectra of total fractions from Δ*copI* (A) and *copA* (B) grown microaerobically in the presence of increasing copper concentrations are shown.

Altogether, our data show that the amount of cbb_3 oxidase and photosystem are similarly affected in *copA* and Δ*copI* mutants by copper excess; nonetheless, the mechanisms are different. Indeed, in the *copA* mutant, the cytoplasmic copper accumulation affects heme and bacteriochlorophyll synthesis, while in the Δ*copI* mutant, the periplasmic copper accumulation affects cytochrome *c* biogenesis.

DISCUSSION

The bacterial inner membrane and the periplasm are likely more exposed to copper than the cytoplasm in Gram-negative bacteria. Indeed, copper-requiring proteins in bacteria identified so far are located in these two cell compartments. Copper entry seems to occur via nonspecific importers, which may load the periplasm and cytoplasm with copper; in addition, the inner membrane copper efflux P-type ATPase CopA unloads excess cytoplasmic copper in the periplasm. Therefore, detoxification of Cu(I) within the periplasm is crucial to preserve the integrity of the membrane and the cell. In *E. coli*, this is accomplished by the periplasmic CueO oxidase and the CusF chaperone, which delivers copper to the Cus efflux system (8). In *Cupriavidus*, this involves many chaperones, such as CopH and CopK. In *Salmonella*, the periplasmic protein CueP seems to be involved in copper sequestration within the periplasm. Finally, in *P. aeruginosa*, periplasmic proteins such as PA2807, PA2808, and azurin are induced by copper and seem to be involved in copper handling within the periplasm (32, 33).

Copper can affect different pathways when it is accumulated in the cytoplasm (1, 25, 34). When present in the membrane or the periplasm, excess copper seems to affect proteins and lipids (35). In this study, we identified CopI, a periplasmic protein present in many bacteria (see Fig. S4 in the supplemental material), and used the corresponding null mutant to identify the pathway(s) damaged by accumulation of excess copper in this compartment. CopI is induced by excess copper and is required for copper tolerance. The mutant lacking CopI is even more sensitive to copper than the ATPase *copA* mutant under microaerobic and anaerobic photosynthetic conditions. This supports the idea that the accumulation of copper in the periplasm is more toxic and highlights the importance of copper handling within this compartment. In this study, we have shown that excess copper in the Δ*copI* mutant affects periplasmic (CcpA and cytochrome *c*′) and membrane (photosystem and cytochrome *c* oxidase cbb_3) *c*-type cytochromes. For cbb_3 oxidase, this decrease was directly correlated with a decrease in the amount of cytochrome *c* subunits CcoP and CcoO within the membrane. A less pronounced reduction of the amount of the catalytic subunit CcoN was also observed, but probably as a consequence of CcoP and CcoO decrease. An effect on the photosystem was also observed and was explained by a decrease in the amount of the tetraheme cytochrome *c* subunit PufC. The high susceptibility to copper during photosynthetic growth in the Δ*copI* mutant is consistent with the idea that periplasmic copper is especially toxic to the *c* type cytochromes. Indeed, photosynthetic growth depends, in addition to the photosystem, on the bc_1 cytochrome complex and other soluble *c*-type cytochromes.

The specific decrease of *c*-type cytochromes within the Δ*copI* mutant and even in the WT when challenged with a high copper concentration prompted us to conclude that copper may affect cytochrome *c* biogenesis within the periplasm. Because the cytochrome *c* biogenesis is a periplasmic pathway involving thiol oxidoreductases and the reduction of cysteine residues for the covalent binding of heme *b* (31), one can envision that copper, a potent oxidant, could interfere with cysteines and/or the reduction system of the cytochrome *c* biogenesis pathway in all organisms. In this respect, it was reported that copper stress in *E. coli* induces periplasmic disulfide bond formation under aerobic conditions and that copper catalyzes the formation of disulfide-bonded oligomers *in vitro* (36). This is the first report that copper should affect a key process in all organisms: the cytochrome *c* biogenesis. Overall, we assume that CopI is an important defense against copper in the periplasm and may protect not only *c* type cytochromes but also other proteins with cysteine residues from copper ions that may catalyze nonnative disulfide bond formation.

In comparison with the Δ*copI* mutant, the copper ATPase *copA* mutant exhibited a comparable phenotype, with a decrease in the photosystem and the cytochrome *c* oxidase cbb_3. We have also found a decrease in the amount of the cbb_3 subunits CcoP and CcoO. In contrast to the Δ*copI* mutant, the tetrapyrrole biosynthesis pathway is affected only in the *copA* mutant, as evidenced by the release of coproporphyrinogen III, due to the accumulation of copper within the cytoplasm in this mutant (25) (Fig. 5B and C). Consequently, production of heme and chlorophylls is reduced in the *copA* mutant, which in turn affects the assembly and/or stability of membrane complexes requiring these cofactors. In the Δ*copI* mutant, these cytoplasmic processes are unaffected and functional because excess copper is transferred to the periplasm by CopA. This is proved by the fact that the Δ*copI* mutant grown in the presence of excess copper does not accumulate or release coproporphyrinogen III in the medium (Fig. 5B and C) and has undiminished succinate dehydrogenase activity (Fig. 7A).

MATERIALS AND METHODS

Bacterial strains and growth media. *E. coli* was grown at 37°C in LB medium. *R. gelatinosus* was grown at 30°C, either microaerobically in the dark (250-ml flasks filled with 250 ml medium) or anaerobically in light (photosynthesis in filled and sealed tubes) on malate growth medium (30). Anaerobic growth on plates was performed using sealed bags with H_2- and CO_2-producing gas packs (Anaerocult P; Merck). Kanamycin, ampicillin, and trimethoprim were used at 50 μg/ml, and tetracycline was used at 1 μg/ml. The malate medium copper concentration is 1.6 μM, and exogenous $CuSO_4$, was added to the growth medium at different concentrations. Bacterial strains and plasmids are listed in Table S1 in the supplemental material. For growth inhibition by $CuSO_4$, cells were grown overnight in liquid medium, diluted 1:100 in the same medium with various copper concentrations, and incubated for 48 h at 30°C under aerobic respiration or anaerobic photosynthesis. Growth was monitored by absorbance at 680 nm.

Molecular biology techniques. Standard methods were performed according to the work of Sambrook et al. (37) unless indicated otherwise.

Gene cloning and plasmid constructions for allele replacement. To clone the *copI* gene from pB79-1 genomic DNA of *R. gelatinosus*, a 2-kb fragment was amplified by PCR using the primers copIF (5′ AGATGAT CCGCCACTACGAGCGC 3′) and copIR (5′-CGTCGATCAGCTGGAC CTGTCGT-3′). Each fragment was cloned into the PCR cloning vector pDrive to give pSA10. The *copI* gene was inactivated by the insertion either of the Km or Tp cassette at the SmaI site. Briefly, plasmid pSA10 was subjected to SmaI restriction enzyme digestion and then ligated with the 0.7-kb SmaI-digested Tp or 1.2-kb MscI Km cassette. The resulting recombinant plasmids were designated pSA20 (*copI*::Km) and pSA21 (*copI*::Tp).

Gene transfer and strain selection. Transformation of *R. gelatinosus* cells was performed by electroporation (38). Transformants were selected on plates supplemented with the appropriate antibiotic under aerobic conditions. Following selection, template genomic DNA was prepared from the ampicillin-sensitive transformants, and the antibiotic resistance marker's presence at the desired locus was confirmed by PCR.

Membrane and soluble protein preparation. The cell extracts were prepared by cell disruption with a French press in 0.1 M sodium phosphate buffer (pH 7.4) containing 1 mM phenylmethylsulfonyl fluoride (PMSF), followed by differential ultracentrifugations as described in reference 5. The resulting pellet (membranes) was resuspended in the same buffer without PMSF, and the supernatant (soluble fraction) was also saved. Protein concentrations were determined using the bicinchoninic acid assay (Sigma) using bovine serum albumin as a standard.

Periplasmic fraction preparation. *R. gelatinosus* cells were washed twice with 50 mM Tris-HCl (pH 7.8) and resuspended in the same buffer in the presence of 0.45 M sucrose, 1.3 mM EDTA, and 0.6 mg/ml lysozyme. After 1 h of incubation at 30°C with soft shaking, the extract was centrifuged for 15 min at 6,000 rpm. The supernatant corresponds to the periplasmic fraction.

RNA extraction and RT-PCR. Total RNA from WT cells grown photosynthetically under different copper concentrations was extracted according to (39). RT-PCR were performed as described by Azzouzi et al. (25) using primers copI-F (5′ ACCTCGTGCAGTTCCTGAAG 3′) and copI-R (5′ CGACGAAGAAGCTGGAGAAG 3′) and primers ol 539 (5′ G GCAGATGATGGCAAACAAG 3′) and ol 540 (5′ GTGGAGCCACGGC GTATAG 3′) for the *pucB* gene.

Blue-native gel electrophoresis and in-gel activities. Blue-native polyacrylamide gel (BN-PAGE) electrophoresis of β-dodecyl-maltoside (DDM)-solubilized membrane proteins and in-gel Cox activity assays were performed as described in reference 30. Succinate dehydrogenase in-gel activity assays were performed as described for the succinate-NBT (Nitroblue tetrazolium) reductase assay in reference 40.

Western blotting and immunodetection. Twenty micrograms (for cbb_3 subunits detection) or 40 μg (for CopA_His_6 detection) of total protein was separated by SDS-PAGE (10, 12, or 13% polyacrylamide) and then transferred to an enhanced chemiluminescence polyvinylidene difluoride membrane (Hybond; GE Healthcare). Before loading, samples were treated 10 min at 37°C for CcoN detection, 5 min at 75°C for CcoO and CcoP detection, or 5 min at 95°C for CopA-His_6 and CopI detection. Membranes were probed with different primary antibodies: anti-CcoN (dilution, 1:1,000), anti-CcoO (dilution, 1:10,000), anti-CcoP (dilution 1:5,000). Secondary horseradish peroxidase (HRP)-conjugated goat anti-rabbit antibody (BioRad) was used at a 1:5,000 dilution. For the detection of CopA-His_6 and CopI, HisProbe-HRP (Pierce) was used according to the manufacturer's instructions. Reactive bands were detected using a chemiluminescent HRP substrate according to the method of Haan and Behrmann (41). Image capture was performed with a LAS-3000 cooled charge-coupled device (CCD) camera system (Fuji).

MICS-BN-PAGE and copper detection PAGE. The procedure for metal ion contaminant sweeping (MICS)-BN-PAGE and copper detection PAGE was performed as reported previously by Saito et al. (29). The procedure is described briefly as follows. A separation gel (10% polyacrylamide, 190 mM Tris-HCl [pH 8.8]) and an upper stacking gel (3.9% polyacrylamide, 63 mM Tris-HCl [pH 7.4]), with the addition of 10 μM EDTA, were prepared for MICS-BN-PAGE. Before sample injection, the gel was conditioned by applying voltage with an upper and lower migration buffer solution including 10 μM TPEN [N,N,N′,N′-tetrakis(2-pyridylmethyl)ethylenediamine] and 10 μM CyDTA (trans-1,2-diaminocyclohexane-N,N,N′,N′-tetraacetic acid monohydrate), respectively, in order to sweep all contaminant metal ions for preparing a metal-free stacking gel. Samples (soluble fractions from the WT and Δ*copI* mutant incubated with the addition of 1.6 or 200 μM $CuSO_4$) were prepared by mixing with 6.3% glycerol, Tris-HCl buffer (pH 7.4), and 3.0 mM CBB (Coomassie Brilliant Blue) G-250. Samples were then loaded into the wells after a rinsing to remove all TPEN and exchange of the upper buffer solution with a Tris-Gly buffer solution without TPEN. A voltage of 600 V was then applied for 3 min to move the sample proteins into the concentration gel. Subsequently, electrophoresis (protein separation) was conducted after exchanging an upper buffer solution with 10 μM TPEN until CBB G-250 migrated to a distance of ~3 to 4 cm. The temperature of the slab gel was kept constant at 273 K.

The separation gel was cut at intervals of 0.25 cm prior to acid extraction of copper ions bound to proteins. Extraction was achieved by shaking the gel fraction with 0.2 M pure hydrochloride solution. Thereafter, the extract was mixed with a solution of the fluorescent probe FTC-ABDOTA (50 μM, 1 μl) in Tris-HCl buffer, to form the Cu^{2+}-FTC-ABDOTA emissive complex for copper detection PAGE. The prepared sample solution was loaded into the well in the second-dimension gel (10% and 30% polyacrylamide for stacking and separation gels, respectively), followed by electrophoresis for separation of copper complexes. The copper bands were detected by fluorescence using a CCD camera (Atto) with a photodiode excitation light source (Invitrogen).

In-gel cytochrome *c* detection. Detection of cytochrome *c* on nonreducing SDS-PAGE was performed using 3,3′,5,5′-tetramethylbenzidine (TMBZ) as described by Thomas et al. (42).

Spectrophotometric measurements. Absorption spectroscopy was performed with a Cary 500 spectrophotometer. For difference (reduced minus oxidized) spectra, total pigments were extracted from cell pellets or membranes with acetone-methanol (7/2 [vol/vol]). For each sample, the spectrum was collected on oxidized sample upon addition of 50 μM $K_6Fe(CN)_3$, the sample was reduced by addition of dithionite (few crystals), and the spectrum was collected to generate the reduced minus oxidized spectrum.

Mass spectrometry analyses. Peptide mixtures generated by standard in-gel digestion with trypsin (Gold; Promega) were SpeedVac treated for 10 min and then analyzed with a quadrupole time-of-flight (QTOF) Premier mass spectrometer coupled to a Acquity nano-ultraperformance liquid chromatograph equipped with a trapping column (Symetry C_{18}; 180 μm by 20 mm; 5-μm particle size) and an analytical column (BEH130 C_{18}; 75 μm by 100 mm; 1.7-μm particle size) (Waters). The aqueous solvent (buffer A) was 0.1% formic acid in water, and the organic phase

(buffer B) was 0.1% formic acid in acetonitrile. A 2-to-40% B gradient was set for 25 min. For exact mass measurements, glufibrinopeptide reference (*m/z* 785.8426) was continuously supplied during nano-liquid chromatography-MS/MS analyses using the lock spray device. Peptide mass measurements were corrected during data processing, and peak lists were generated by PLGS (ProteinLynx Global Server; Waters). Processed data were submitted to Mascot searching using the following parameters: data bank, NCBInr; taxonomy, bacteria; peptide tolerance, 20 ppm; fragment tolerance, 0.1 Da; digestion, reagent trypsin; variable modification, oxidation (methionine); fixed modification, carbamido-methylation (cysteine). Validation criteria for protein identification were two peptides with a Mascot individual ion score of >43.

Nucleotide sequence accession number. The *copI* and *copJ* sequences reported in this paper were deposited in GenBank (accession number KF938602.1).

SUPPLEMENTAL MATERIAL

Supplemental material for this article may be found at http://mbio.asm.org/lookup/suppl/doi:10.1128/mBio.01007-15/-/DCSupplemental.

Figure S1, PDF file, 0.1 MB.
Figure S2, PDF file, 0.1 MB.
Figure S3, PDF file, 0.1 MB.
Figure S4, PDF file, 0.5 MB.
Table S1, DOC file, 0.04 MB.

ACKNOWLEDGMENTS

We are grateful to Jérome Leconte for his help with sequence analyses and to Monique Rougeot for the reading of the manuscript. This work has benefited from the facilities and expertise of the SICaPS platform of I2BC (Institut de Biologie Intégrative de la Cellule).

REFERENCES

1. **Macomber L, Imlay JA**. 2009. The iron-sulfur clusters of dehydratases are primary intracellular targets of copper toxicity. Proc Natl Acad Sci U S A **106:**8344–8349. http://dx.doi.org/10.1073/pnas.0812808106.
2. **Tan G, Cheng Z, Pang Y, Landry AP, Li J, Lu J, Ding H**. 2014. Copper binding in IscA inhibits iron-sulphur cluster assembly in *Escherichia coli*. Mol Microbiol **93:**629–644. http://dx.doi.org/10.1111/mmi.12676.
3. **Nies DH, Herzberg M**. 2013. A fresh view of the cell biology of copper in enterobacteria. Mol Microbiol **87:**447–454. http://dx.doi.org/10.1111/mmi.12123.
4. **González-Guerrero M, Raimunda D, Cheng X, Argüello JM**. 2010. Distinct functional roles of homologous Cu+ efflux ATPases in *Pseudomonas aeruginosa*. Mol Microbiol **78:**1246–1258. http://dx.doi.org/10.1111/j.1365-2958.2010.07402.x.
5. **Hassani BK, Astier C, Nitschke W, Ouchane S**. 2010. CtpA, a copper-translocating P-type ATPase involved in the biogenesis of multiple copper-requiring enzymes. J Biol Chem **285:**19330–19337. http://dx.doi.org/10.1074/jbc.M110.116020.
6. **Koch HG, Winterstein C, Saribas AS, Alben JO, Daldal F**. 2000. Roles of the ccoGHIS gene products in the biogenesis of the cbb(3)-type cytochrome *c* oxidase. J Mol Biol **297:**49–65. http://dx.doi.org/10.1006/jmbi.2000.3555.
7. **Outten FW, Outten CE, Hale J, O'Halloran TV**. 2000. Transcriptional activation of an *Escherichia coli* copper efflux regulon by the chromosomal MerR homologue, cueR. J Biol Chem **275:**31024–31029. http://dx.doi.org/10.1074/jbc.M006508200.
8. **Rensing C, Grass G**. 2003. *Escherichia coli* mechanisms of copper homeostasis in a changing environment. FEMS Microbiol Rev **27:**197–213. http://dx.doi.org/10.1016/S0168-6445(03)00049-4.
9. **Rensing C, Fan B, Sharma R, Mitra B, Rosen BP**. 2000. CopA: an *Escherichia coli* Cu(I)-translocating P-type ATPase. Proc Natl Acad Sci U S A **97:**652–656. http://dx.doi.org/10.1073/pnas.97.2.652.
10. **Roberts SA, Weichsel A, Grass G, Thakali K, Hazzard JT, Tollin G, Rensing C, Montfort WR**. 2002. Crystal structure and electron transfer kinetics of CueO, a multicopper oxidase required for copper homeostasis in *Escherichia coli*. Proc Natl Acad Sci U S A **99:**2766–2771. http://dx.doi.org/10.1073/pnas.052710499.
11. **Long F, Su CC, Lei HT, Bolla JR, Do SV, Yu EW**. 2012. Structure and mechanism of the tripartite CusCBA heavy-metal efflux complex. Philos Trans R Soc Lond B Biol Sci **367:**1047–1058. http://dx.doi.org/10.1098/rstb.2011.0203.
12. **Outten FW, Huffman DL, Hale JA, O'Halloran TV**. 2001. The independent cue and cus systems confer copper tolerance during aerobic and anaerobic growth in *Escherichia coli*. J Biol Chem **276:**30670–30677. http://dx.doi.org/10.1074/jbc.M104122200.
13. **Raimunda D, González-Guerrero M, Leeber BW III, Argüello JM**. 2011. The transport mechanism of bacterial Cu+-ATPases: distinct efflux rates adapted to different function. Biometals **24:**467–475. http://dx.doi.org/10.1007/s10534-010-9404-3.
14. **Lee SM, Grass G, Rensing C, Barrett SR, Yates CJ, Stoyanov JV, Brown NL**. 2002. The Pco proteins are involved in periplasmic copper handling in *Escherichia coli*. Biochem Biophys Res Commun **295:**616–620. http://dx.doi.org/10.1016/S0006-291X(02)00726-X.
15. **Bersch B, Favier A, Schanda P, van Aelst S, Vallaeys T, Covès J, Mergeay M, Wattiez R**. 2008. Molecular structure and metal-binding properties of the periplasmic CopK protein expressed in *Cupriavidus metallidurans* CH34 during copper challenge. J Mol Biol **380:**386–403. http://dx.doi.org/10.1016/j.jmb.2008.05.017.
16. **Von Rozycki T, Nies DH**. 2009. *Cupriavidus metallidurans*: evolution of a metal-resistant bacterium. Antonie Van Leeuwenhoek **96:**115–139. http://dx.doi.org/10.1007/s10482-008-9284-5.
17. **Osman D, Waldron KJ, Denton H, Taylor CM, Grant AJ, Mastroeni P, Robinson NJ, Cavet JS**. 2010. Copper homeostasis in *Salmonella* is atypical and copper-CueP is a major periplasmic metal complex. J Biol Chem **285:**25259–25268. http://dx.doi.org/10.1074/jbc.M110.145953.
18. **Pontel LB, Soncini FC**. 2009. Alternative periplasmic copper-resistance mechanisms in gram negative bacteria. Mol Microbiol **73:**212–225. http://dx.doi.org/10.1111/j.1365-2958.2009.06763.x.
19. **Quaranta D, McCarty R, Bandarian V, Rensing C**. 2007. The copper-inducible cin operon encodes an unusual methionine-rich azurin-like protein and a pre-Q0 reductase in *Pseudomonas putida* KT2440. J Bacteriol **189:**5361–5371. http://dx.doi.org/10.1128/JB.00377-07.
20. **Giner-Lamia J, Lopez-Maury L, Florencio FJ**. 2015. CopM is a novel copper-binding protein involved in copper resistance in *Synechocystis sp*. PCC 6803. Microbiologyopen **4:**167–185. http://dx.doi.org/10.1002/mbo3.231
21. **Waldron KJ, Firbank SJ, Dainty SJ, Pérez-Rama M, Tottey S, Robinson NJ**. 2010. Structure and metal loading of a soluble periplasm cuproprotein. J Biol Chem **285:**32504–32511. http://dx.doi.org/10.1074/jbc.M110.153080.
22. **Lim SY, Joe MH, Song SS, Lee MH, Foster JW, Park YK, Choi SY, Lee IS**. 2002. CuiD is a crucial gene for survival at high copper environment in *Salmonella enterica serovar typhimurium*. Mol Cells **14:**177–184.
23. **Wiethaus J, Wildner GF, Masepohl B**. 2006. The multicopper oxidase CutO confers copper tolerance to *Rhodobacter capsulatus*. FEMS Microbiol Lett **256:**67–74. http://dx.doi.org/10.1111/j.1574-6968.2005.00094.x.
24. **Peuser V, Glaeser J, Klug G**. 2011. The RSP_2889 gene product of *Rhodobacter sphaeroides* is a CueR homologue controlling copper-responsive genes. Microbiology **157:**3306–3313. http://dx.doi.org/10.1099/mic.0.051607-0.
25. **Azzouzi A, Steunou AS, Durand A, Khalfaoui-Hassani B, Bourbon ML, Astier C, Bollivar DW, Ouchane S**. 2013. Coproporphyrin III excretion identifies the anaerobic coproporphyrinogen III oxidase HemN as a copper target in the Cu^{+}-ATPase mutant *copA*− of *Rubrivivax gelatinosus*. Mol Microbiol **88:**339–351. http://dx.doi.org/10.1111/mmi.12188.
26. **Liotenberg S, Steunou AS, Durand A, Bourbon ML, Bollivar D, Hansson M, Astier C, Ouchane S**. 2015. Oxygen-dependent copper toxicity: targets in the chlorophyll biosynthesis pathway identified in the copper efflux ATPase CopA deficient mutant. Environ Microbiol **17:**1963–1976. http://dx.doi.org/10.1111/1462-2920.12733.
27. **Djoko KY, McEwan AG**. 2013. Antimicrobial action of copper is amplified via inhibition of heme biosynthesis. ACS Chem Biol **8:**2217–2223. http://dx.doi.org/10.1021/cb4002443.
28. **Uriu-Adams JY, Keen CL**. 2005. Copper, oxidative stress, and human health. Mol Aspects Med **26:**268–298. http://dx.doi.org/10.1016/j.mam.2005.07.015.
29. **Saito S, Kawashima M, Ohshima H, Enomoto K, Sato M, Yoshimura H, Yoshimoto K, Maeda M, Shibukawa M**. 2013. Separation of metalloproteins using a novel metal ion contaminant sweeping technique and detection of protein-bound copper by a metal ion probe in polyacrylamide gel

electrophoresis: distribution of copper in human serum. Analyst **138:** 6097–6105. http://dx.doi.org/10.1039/c3an01107k.
30. **Hassani BK, Steunou AS, Liotenberg S, Reiss-Husson F, Astier C, Ouchane S**. 2010. Adaptation to oxygen: role of terminal oxidases in photosynthesis initiation in the purple photosynthetic bacterium, *Rubrivivax gelatinosus*. J Biol Chem **285:**19891–19899. http://dx.doi.org/10.1074/jbc.M109.086066.
31. **Sanders C, Turkarslan S, Lee DW, Daldal F**. 2010. Cytochrome *c* biogenesis: the Ccm system. Trends Microbiol **18:**266–274. http://dx.doi.org/10.1016/j.tim.2010.03.006.
32. **Raimunda D, Padilla-Benavides T, Vogt S, Boutigny S, Tomkinson KN, Finney LA, Argüello JM**. 2013. Periplasmic response upon disruption of transmembrane Cu transport in *Pseudomonas aeruginosa*. Metallomics **5:**144–151. http://dx.doi.org/10.1039/c2mt20191g.
33. **Teitzel GM, Geddie A, De Long SK, Kirisits MJ, Whiteley M, Parsek MR**. 2006. Survival and growth in the presence of elevated copper: transcriptional profiling of copper-stressed *Pseudomonas aeruginosa*. J Bacteriol **188:**7242–7256. http://dx.doi.org/10.1128/JB.00837-06.
34. **Yoon BY, Kim JS, Um SH, Jo I, Yoo JW, Lee K, Kim YH, Ha NC**. 2014. Periplasmic disulfide isomerase DsbC is involved in the reduction of copper binding protein CueP from *Salmonella enterica serovar typhimurium*. Biochem Biophys Res Commun **446:**971–976. http://dx.doi.org/10.1016/j.bbrc.2014.03.043.
35. **Hong R, Kang TY, Michels CA, Gadura N**. 2012. Membrane lipid peroxidation in copper alloy-mediated contact killing of *Escherichia coli*. Appl Environ Microbiol **78:**1776–1784. http://dx.doi.org/10.1128/AEM.07068-11.
36. **Hiniker A, Collet JF, Bardwell JC**. 2005. Copper stress causes an in vivo requirement for the *Escherichia coli* disulfide isomerase DsbC. J Biol Chem **280:**33785–33791. http://dx.doi.org/10.1074/jbc.M505742200.
37. **Sambrook J, Fritsch EF, Maniatis T**. 1989. Molecular cloning: a laboratory manual, 2nd ed. Cold Spring Harbor, NY.
38. **Ouchane S, Picaud M, Reiss-Husson F, Vernotte C, Astier C**. 1996. Development of gene transfer methods for *Rubrivivax gelatinosus* S1: construction, characterization and complementation of a puf operon deletion strain. Mol Gen Genet **252:**379–385. http://dx.doi.org/10.1007/BF02173002.
39. **Steunou AS, Astier C, Ouchane S**. 2004. Regulation of photosynthesis genes in *Rubrivivax gelatinosus*: transcription factor PpsR is involved in both negative and positive control. J Bacteriol **186:**3133–3142. http://dx.doi.org/10.1128/JB.186.10.3133-3142.2004.
40. **Wittig I, Karas M, Schägger H**. 2007. High resolution clear native electrophoresis for in-gel functional assays and fluorescence studies of membrane protein complexes. Mol Cell Proteomics **6:**1215–1225. http://dx.doi.org/10.1074/mcp.M700076-MCP200.
41. **Haan C, Behrmann I**. 2007. A cost effective non-commercial ECL-solution for Western blot detections yielding strong signals and low background. J Immunol Methods **318:**11–19. http://dx.doi.org/10.1016/j.jim.2006.07.027.
42. **Thomas PE, Ryan D, Levin W**. 1976. An improved staining procedure for the detection of the peroxidase activity of cytochrome P-450 on sodium dodecyl sulfate polyacrylamide gels. Anal Biochem **75:**168–176. http://dx.doi.org/10.1016/0003-2697(76)90067-1.